Assembly of Methylene Blue on Nucleic Acid Template as Studied by Resonance Light-Scattering Technique and Determination of Nucleic Acids of Nanogram

Cheng Zhi Huang,* Yuan Fang Li, Shi You Deng, and Shu Rong Liu

Institute of Environmental Chemistry, Southwest Normal University, Chongqing 400715, the People's Republic of China

(Received September 8, 1998)

The template role of nucleic acids in the long-range assembly of Methylene Blue (MB) was characterized with Resonance Light-Scattering (RLS) measurements, and a determination method of nucleic acids of nanogram was proposed. At the pH range 6.87—8.74 and ionic strength lower than 0.01, the interactions of MB with nucleic acids result in two characteristic RLS peaks at 355.0 and 560.0 nm. Mechanism studies show that these peaks result from the long-range assembly of MB on the molecular surface of nucleic acids. A Scatchard plot was constructed by using the RLS data, yielding an assembly number and assembly constant of 5.67 and 9.22×10^4 mol^{-1} dm^3 for MB assembly on the molecular surface of calf thymus DNA (ctDNA), 5.79 and 4.68×10^4 mol^{-1} dm^3 for MB assembly on that of fish sperm DNA (fsDNA). This assembly could be used for analytical purposes and 0—1.4 $\mu g\,ml^{-1}$ for ctDNA, 0—1.2 $\mu g\,ml^{-1}$ for fsDNA, and 0—0.24 $\mu g\,ml^{-1}$ for yeast RNA could be determined if 3.0×10^{-5} $mol\,dm^{-3}$ MB was employed. The limits of determination were 11.0 $ng\,ml^{-1}$ for ctDNA, 4.9 $ng\,ml^{-1}$ for fsDNA and 8.6 $ng\,ml^{-1}$ for yeast RNA, respectively. Four synthetic samples were determined with satisfaction.

The study of supramolecular interactions of organic dyes with biological molecules is an increasingly interesting field in recent decades, since these interactions can help to understand the structures and functions of biological macromolecules,[1,2] and can act as study models of some biophysical processes.[3] Based on these interactions, analytical methods of biological macromolecules can be established.[4,5] In terms of the mechanism, the determination method of nucleic acids is established mainly based on two kinds of interactions: One involves the reactions of the components of nucleic acids—phosphorus,[6] bases,[7] or sugar[8] with organic drugs such as diphenylamine,[8] indole,[9] *p*-nitrophenylhydrazine[10] etc.; the other one is based on the resonance energy transfer from nucleic acids to organic dyes, such as ethidium bromide,[11] Hoechst 33258,[12] Yellow Orange dyes.[13—16] Furthermore, trivalent metal ions, such as Tb(III),[17,18] Eu(III),[19] Sc(III),[20—22] Y(III),[21—23] La(III),[21,24] Al(III),[22,25] have been developed as fluorescence probes of the structures and the functions of nucleic acids in recent years.

DNA has long been recognized as an important target for phenothiazinium dye photosensitized biological damage. It has been found that Methylene Blue (MB) damages DNA at guanine residues, which can lead to a subsequent cleavage of DNA upon exposure to alkali.[26] At a low molar ratio of the dye to nucleic acids (*m*), the intercalation of an organic dye into base pairs of nucleic acids is suggested as the preferred binding mode, while at a high *m* ratio of the dye to nucleic acids, aggregation of MB via cooperative stacking outside the helix appears to occur.[26] Photoexcitation of MB when bound at a low *m* ratio leads to rapid deactivation from their singlet states to their ground states via direct reactions with the nucleotide bases. Thus, although direct reactions may give rise to some damage, the singlet oxygen-induced damage to DNA is expected to be minimal. At a high *m* ratio, however, weak cooperative binding occurs under conditions where the dye is in excess, which is suggested to be external stacking of the dye molecules promoted by polyanion;[26] in such a case, a significant concentration of the dye remains free in solution, and is expected to produce singlet oxygen, which can attack and readily damage DNA.[27]

Herein, we report on the external stacking of MB promoted by nucleic acid polyanion at a high *m* ratio, based on resonance light-scattering (RLS) measurements; accordingly, a determination method of nucleic acids is proposed. The RLS technique has been extensively studied and applied to solve many problems in recent years.[28—35] According to macroscopic fluctuation theory,[28] scattering light originates from fluctuations of the solution refractive index, which consists of real and imaginary parts. In a transparent isotropic medium, since the imaginary part of the refractive index originating from the molecular absorption can be neglected, the Rayleigh-scattering law is obeyed for the light-scattering of the molecular particles with a size 20-fold smaller than the wavelength of the incident beam.[28] However, if the wavelength of the incident beam is close to that of the absorption band of the molecular particles, which exist as aggregates, enhanced Rayleigh light-scattering can be expected, because of fluctuation of the imaginary part of the refractive index, which may be comparable to that of the real part of the refractive index.[28] The enhanced Rayleigh light-

scattering of aggregated molecules can be detected, even by using a common spectrofluorometer.[29,30] However, the resonance signals of light-scattering detected by using the spectrofluorometer are made up of several light-scattering components, such as Rayleigh light-scattering, Tyndall light-scattering and dynamic light-scattering.[31] Even though, an enhanced intensity of resonance light-scattering (RLS) was found to be proportional to the concentration of the aggregated molecules, if the instrumental conditions of the spectrofluorometer were adjusted without marked variations.[32—36] Since all of the absorption processes are inherently associated with light-scattering, it is possible that the weak RLS of organic dyes can be enhanced through their binding with macromolecules, such as nucleic acids and proteins. Thus, by using the RLS technique, we have developed sensitive methods for trace amounts of nucleic acids[32—34] and proteins[35,36] in synthetic[32—34] and practical[35,36] samples, monitored the formation of the suprahelical helixes of nucleic acids[37,38] and established an aggregation mechanism of porphyrins in the presence of proteins[39] and surfactants.[40]

In this report, the external stacking of MB promoted by nucleic acid polyanion results in two characteristic peaks of RLS at 355.0, and 560.0 nm in the pH range 6.87—8.74 and at ionic strength lower than 0.01. The enhanced intensity of RLS at 355.0 nm is proportional to the concentration of nucleic acids. With that, nucleic acids of nanogram amount can be determined.

Experimental

Apparatus. The RLS spectrum and intensity were measured with a Shimadzu RF-540 spectrofluorometer (Kyoto, Japan), while the absorption spectrum was measured using a Hitachi U-3400 Spectrophotometer (Tokyo, Japan). A pH S-10A digital pH meter (Xiaoshan Scientific Instruments Plant, Zhejiang, China) was used to measure the pH values of the solutions, and an MVS-1 vortex mixer (Beide Scientific Instrumental Ltd., Beijing, China) was used to blend the solutions in volumetric flasks.

Reagents. Stock solutions of DNAs and RNA were prepared by dissolving commercially purchased calf thymus DNA (Beitai Biochemical Co., Chinese Academy of Sciences, Beijing, China), fish sperm DNA and yeast RNA (Shanghai Institute of Biochemistry, Chinese Academy of Sciences, Shanghai, China) in doubly distilled water. For DNAs, 24 h or more were needed at 4 °C, with occasional gentle shaking. The concentrations of nucleic acids were determined according to the absorbances at 260 nm after establishing that the absorbance ratio (A_{260}/A_{280}) was in the range 1.80—1.90 for DNAs and 1.90—2.00 for yRNA. The molarities of nucleic acids, when necessary, were calculated using ε_{DNA} = 6600 $dm^3\ mol^{-1}\ cm^{-1}$ and ε_{RNA} = 7800 $dm^3\ mol^{-1}\ cm^{-1}$, respectively.[41] The working solutions of nucleic acids were 1.0 mg ml^{-1} (0.003 mol dm^{-3}), 25.0 μg ml^{-1} (7.5×10^{-5} mol dm^{-3}) and 10.0 μg ml^{-1} (3.0×10^{-5} mol dm^{-3}).

A stock solution of Methylene Blue (MB) was prepared by dissolving the crystallized product (The Third Chemical Reagent Plant of Shanghai, Shanghai, China) in doubly distilled water. Its working solution was 2.0×10^{-4} mol dm^{-3}.

A Tris-HCl buffer (pH 8.14) and Britton–Robinson buffer solution (pH 3.72—8.73) were used to control the acidity, while a 1.0 mol dm^{-3} NaCl solution was used to adjust the ionic strength of the aqueous solutions.

All other reagents were of analytical-reagent grade without further purification. Doubly distilled water was used throughout.

Samples. To test the determination, four synthetic samples containing nucleic acids were constructed by mixing a standard nucleic acid solution with foreigh substances with their concentrations below the tolerance level of the method to the coexisting substances.

Procedure. Into a 10-ml volumetric flask were added appropriate working solution, or a sample solution composing nucleic acids, and a 1.0 ml of buffer solution; after the resulting solution was vortexed, a 1.50 ml of MB solution was added. The mixture was at last diluted to 10 ml using doubly distilled water, and was then mixed thoroughly. All of the absorption and RLS measurements were obtained against a blank treated in the same way without nucleic acids.

The spectrum of RLS was obtained according to the literature.[29—33] The main procedure was to simultaneously scan the excitation and emission monochromator of the RF-540 spectrofluorometer over the wavelength range from 250 to 650 nm with $\Delta\lambda$ = 0 nm. The intensity of RLS was measured at the maximum wavelength. The 150-W xenon, which was equipped in the spectrofluorometer, was adjusted with constant geometry throughout the scanning process and the determination. All of the data were obtained with 5.0 nm of the slit-width for the excitation and emission.

Results and discussion

Resonance Light-Scattering Spectrum. Figure 1 shows that MB has a weak RLS in the region 320 to 550 nm, accompanying an *overshoot* peak at 472 nm; even though, RLS in the region less than 320 nm and higher than 550 nm are much weaker. If a ctDNA solution was added to the

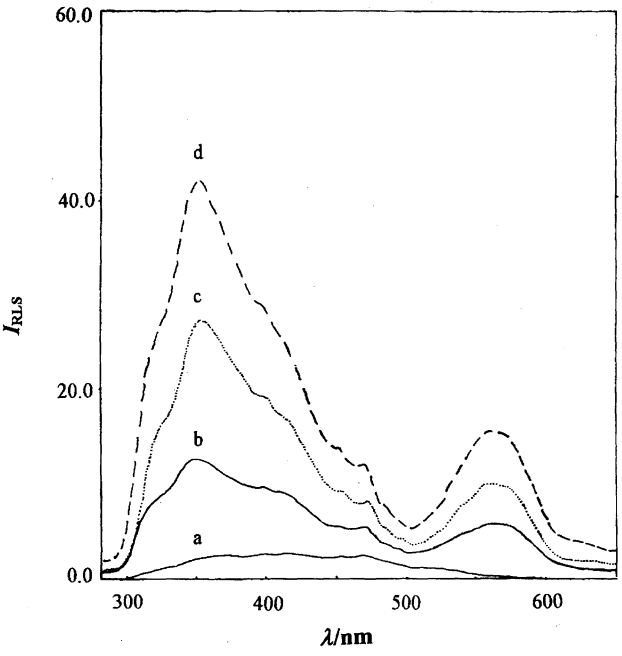

Fig. 1. The RLS spectra of MB in the absence (a) and presence (b—d) of ctDNA. Concentrations: MB, 3.0×10^{-5} mol dm^{-3}; ctDNA (μg ml^{-1}): a, 0.0; b, 0.4; c, 0.8; d, 1.2. pH 8.14. Ionic strength 0.006. All pH values of the medium was controlled by using Tris-HCl buffer solution except being specified.

MB system, however, two enhanced RLS peaks could be observed at 355.0 and 560.0 nm with a shoulder peak at 472 nm (Fig. 1). The intensities of these RLS signals increase with increasing ctDNA concentration. Similar RLS spectra could be obtained for the interactions of MB with fsDNA or yRNA.

It was found that ctDNA has a weak RLS when its concentration is lower than 50 $\mu g\,ml^{-1}$ (Fig. 2). With increasing the MB concentration, RLS signals in the range 308—550 nm increase, while those in the range higher than 550 nm increase initially and then decrease with the turning point at the molar ratio of MB to ctDNA (m) being 6.7, accompanying a few nanometers' blue-shift of the RLS peak at 560 nm. Comparedly, the RLS signals in the range lower than 308 nm decrease all the time with increasing MB concentration, leading to an equal light-scattering point at 308.0 nm.

Since the enhancement of RLS is always associated with aggregation, and depends sensitively on the electronic properties of the individual chromophores, the extent of the electric coupling among chromophores and the size of the aggregate formed, it is important to observe the molecular absorption features of MB and MB–ctDNA complex in order to understand the interaction mechanism. Figure 3 shows that MB has three absorption bands at 292.5, 616.0, and 664.0 nm, accompanying a shoulder peak at 327.5 nm. Since it was found that the absorption both at 664.0 and 290.0 nm does not follow Beer's law if the MB concentration is higher than 1.6×10^{-5} mol dm^{-3}, it is possible that MB has aggregation tendency in the testing medium with increasing its concentration. By calculating the absorbance ratio at 664.0 with 616.0 nm, and that at 292.5 with 327.5 nm, it was found that

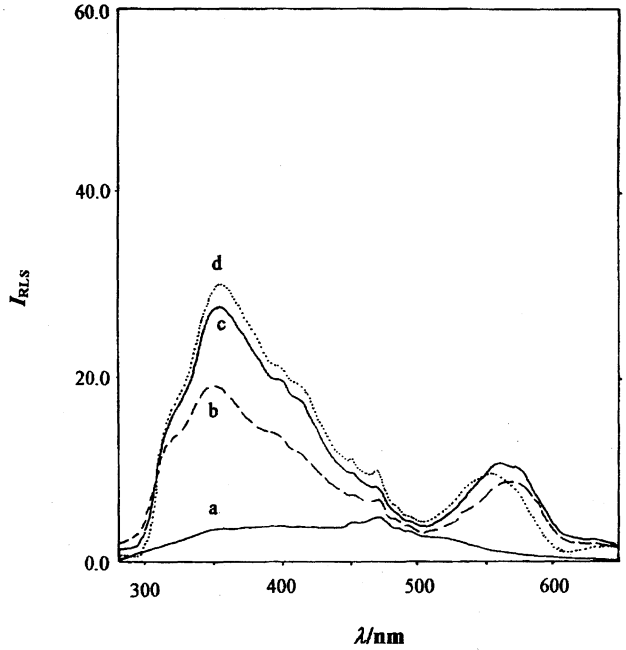

Fig. 2. The effects of the concentration of MB on the RLS spectra of the interaction of MB with ctDNA. Concentrations: MB ($\times10^{-5}$ mol dm^{-3}): a, 0.0; b, 2.0; c, 3.0; d, 4.0; ctDNA, 0.80 $\mu g\,ml^{-1}$. pH 8.14. Ionic strength 0.006.

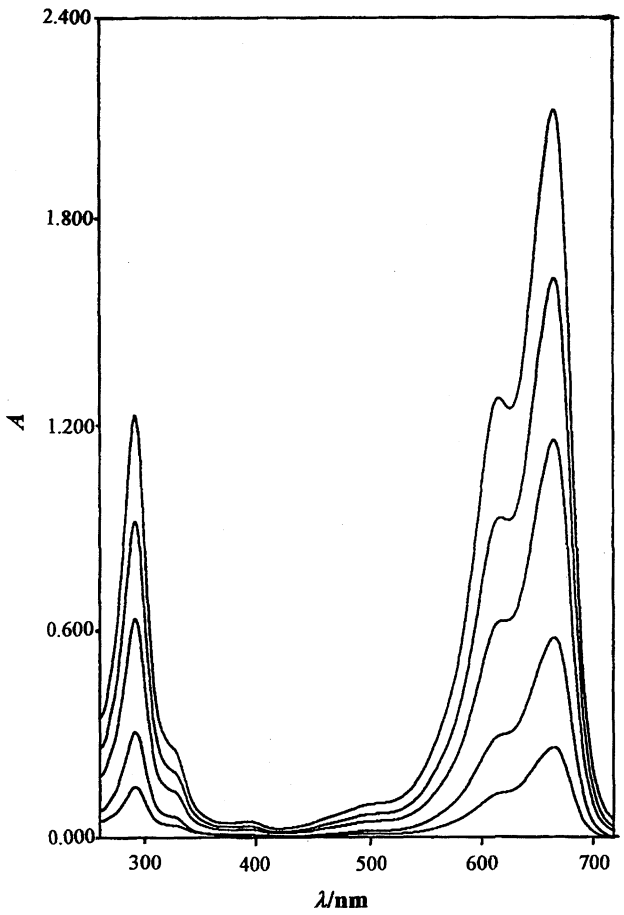

Fig. 3. The ***H***- and ***J***-aggregation of MB with its concentration increasing. Concentration of MB (from bottom to top, $\times10^{-5}$ mol dm^{-3}): 0.4; 0.8; 1.6; 2.4; 3.2. pH: 8.14; Ionic strength, 0.006.

since these absorbance ratios decrease with increasing MB concentration (Table 1), the 616.0 and 327.5 nm absorption bands originate from aggregations of the species which are responsible for the absorption bands at the 664.0 and 292.5 nm band, respectively. As a matter of fact, the 616 nm band originates from ***H***-aggregation of the 664.0 nm band because the band of aggregation (616.0 nm) locates on the blue side of the 664.0 nm band, while the shoulder peak at the 327.5 nm band originates from the ***J***-aggregation of the 292.5 nm band, because the band of aggregation is located on the red side of the 292.5 nm band.[42,43] Similar to the aggregation of porphyrins,[39,40,43] the ***J***-aggregate can be viewed

Table 1. The Absorbance Ratio of the Characteristic Band of MB

MB concentration/10^{-5} mol dm^{-3}	$\frac{A_{664.0\ nm}}{A_{616.0\ nm}}$	$\frac{A_{292.5\ nm}}{A_{327.5\ nm}}$
0.4	2.690	5.000
0.8	1.944	4.947
1.6	1.837	4.825
2.4	1.750	4.817
3.2	1.660	4.774

pH: 8.14; Ionic strength, 0.006.

as forming a linear staggering card-deck structure, which is caused by a hydrophobic attraction due to an intermolecular charge-resonance interaction between the filled and vacant frontier orbitals of neighboring MB molecules in the ground state. The ***H***-aggregate, however, can be viewed as being a stacking card-deck arrangement, which decreases the interaction distance, leading to a blue-shifted absorption band.[40] As Fig. 3 and Table 1 show, both ***J***- and ***H***-aggregations are encouraged by increasing the MB concentration.

When a ctDNA solution was added to an MB solution in which ***J***- and ***H***-aggregations occurred, a hypochromic effect could be observed (Fig. 4), producing a new weak absorption band at about 570 nm. Since an isosbestic point can be observed at 585.0 nm if $m \geq 2.5$, it is reasonable to establish the interaction mechanism of MB with nucleic acids, producing a new complex, MB–ctDNA; however, the absorption spectra do not cross the isosbestic point if $m \leq 2.5$.

Herein occurs one problem, that both ***J***- and ***H***-aggregations of MB have weak RLS signals (Fig. 1a), while the MB–ctDNA complex has strong RLS signals (Figs. 1b and 1c). By analyzing the Scatchard plot, we can understand the interaction mechanism better.

Scatchard Plot of the Binding of MB with Nucleic Acids. A Scatchard plot is commonly used to discuss the interactions of organic dyes with macromolecules. The data for a Scatchard plot usually come from measurements of the absorbance or fluorescence, and the common case is a low R value (R definition will be displayed next).[2] Herein, by using RLS data, we can investigate the interaction of MB with nucleic acids at high R values.

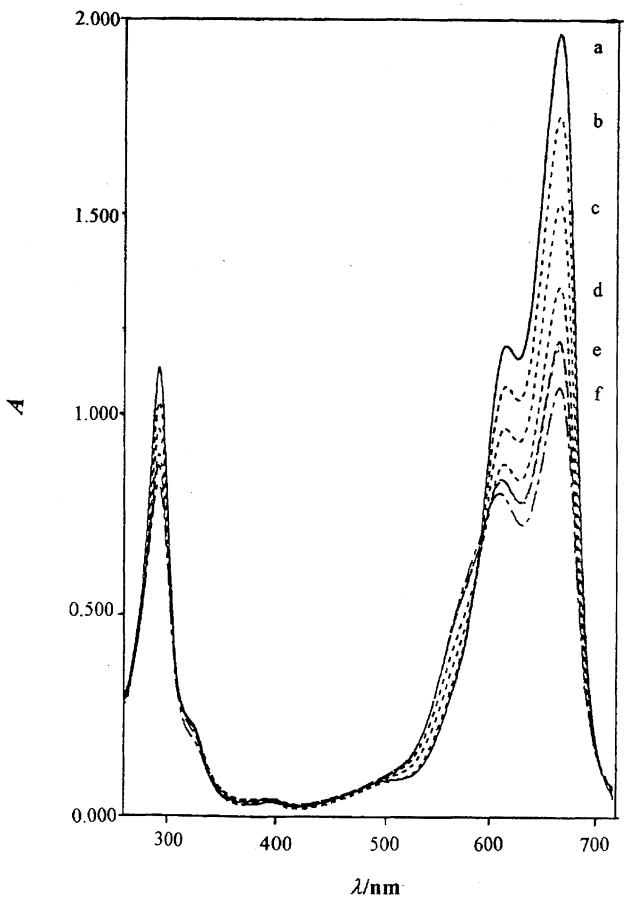

Fig. 4. The absorption spectra of the interaction of MB with calf thymus DNA. Concentrations: MB, 3.0×10^{-5} mol dm^{-3}; ctDNA (μg ml^{-1}): a, 0.0; b, 1.0; c, 2.0; d, 3.0; e, 4.0; f, 5.0. pH 8.14. Ionic strength 0.006.

The binding equilibrium of MB with nucleic acids may be described in terms of the Scatchard equation,[44]

$$\frac{R}{[\mathrm{MB}]} = nK - RK, \tag{1}$$

where R is the molar ratio of bound MB to the base-pair concentration of nucleic acids; n is the maximum value of R; K is the intrinsic binding constant of MB to nucleic acids; and [MB] is the equilibrium concentration of MB, which can be determined by using $[\mathrm{MB}] = c_{\mathrm{MB}} - [\mathrm{MB{\cdot}NA}]$. In the [MB] expression equation, c_{MB} is the total MB concentration and [MB·NA] is the bound concentration of MB, which can be determined by monitoring I_{RLS} according to following equation if c_{MB} is controlled:

$$[\mathrm{MB{\cdot}NA}] = \frac{I_{\mathrm{RLS}} - k_{\mathrm{MB}} c_{\mathrm{MB}}}{k_{\mathrm{MB{\cdot}NA}} - k_{\mathrm{MB}}}. \tag{2}$$

Here I_{RLS} is the intensity of RLS, and is equal to the sum of the intensities of the species in the solution,

$$I_{\mathrm{RLS}} = I_{\mathrm{MB}} + I_{\mathrm{MB{\cdot}NA}}. \tag{3}$$

Both I_{MB}, the intensity of RLS of free MB, and $I_{\mathrm{MB{\cdot}NA}}$, the intensity of MB bound to nucleic acids, are functions of the concentration of unbound MB ([MB]) and bound MB ([MB·NA]). If the concentration of MB is lower than 1.6×10^{-5} mol dm^{-3}, namely the absorption of MB follows Beer's law and MB has not significant aggregation,

$$\begin{aligned} I_{\mathrm{RLS}} &= k_{\mathrm{MB}}[\mathrm{MB}] + k_{\mathrm{MB{\cdot}NA}}[\mathrm{MB{\cdot}NA}] \\ &= k_{\mathrm{MB}}(c_{\mathrm{MB}} - [\mathrm{MB{\cdot}NA}]) + k_{\mathrm{MB{\cdot}NA}}[\mathrm{MB{\cdot}NA}] \end{aligned} \tag{4}$$

The constants, k_{MB} and $k_{\mathrm{MB{\cdot}NA}}$, can be experimentally determined according to Strothkamp and Strothkamp,[45] and then R/[MB] can be calculated in order to construct a Scatchard plot.

Figure 5 shows the results of a Scatchard plot analysis for the interaction of MB with ctDNA and fsDNA, respectively. It is worth noting that Eq. 4 should be correct only in the MB concentration range following Beer's law. If the MB concentrate is too high, namely the R value is large, the Scatchard plot, as Fig. 5 shows, will be curved concave downwards, because a kind of cooperative binding process occurs. From the linear-regression equations for the interactions of MB with ctDNA and fsDNA, which are $R/[\mathrm{MB}] = 521879.8 - 92226.6R$ ($r = -0.9784$), and $R/[\mathrm{MB}] = 271247.9 - 46809.8R$ ($r = -0.9944$), respectively, we can obtain the values of n and K for the interactions of MB when ctDNA are 5.67 and 9.22×10^4 mol^{-1} dm^3; those with fsDNA are 5.79 and 4.68×10^4 mol^{-1} dm^3, respectively.

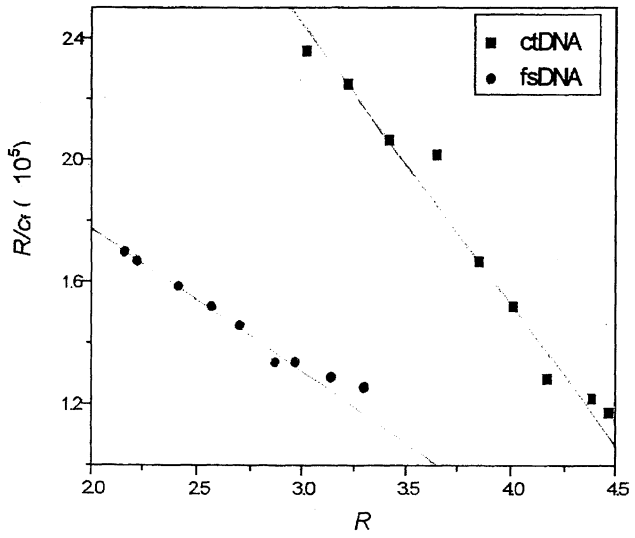

Fig. 5. Scatchard plot of the interaction of MB with ctDNA, fsDNA as measured by RLS. pH 8.14. Ionic strength 0.006.

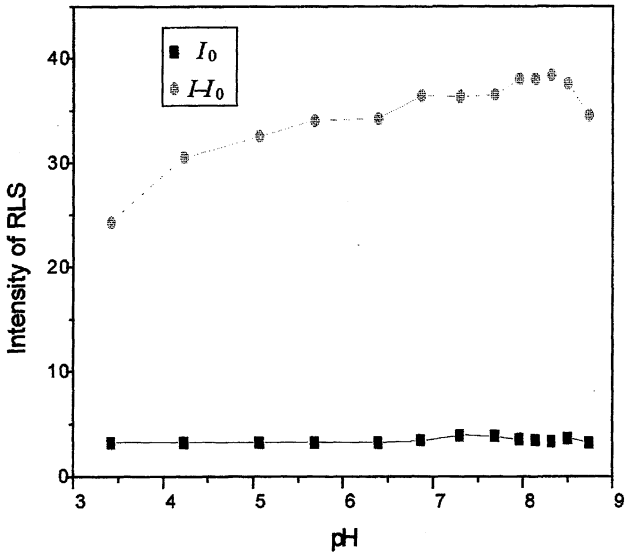

Fig. 6. The effects of pH on the intensity of RLS. Britton–Robinson buffer solution was used. All the data were obtained by adding NaCl solution to adjust the ionic strength as 0.006. MB: 3.0×10^{-5} mol dm^{-3}; ctDNA: 1.0 μg ml^{-1}.

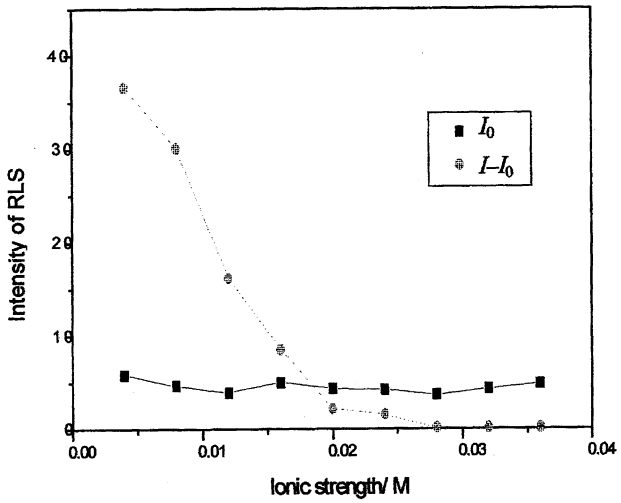

Fig. 7. The effects of ionic strength on the intensity of RLS. Concentrations: MB, 3.0×10^{-5} mol dm^{-3}; ctDNA, 1.0 μg ml^{-1}. pH 8.14.

It is thus reasonable to establish the aggregation mechanism of MB in the presence of ctDNA or fsDNA by using an aggregation number of about 6. This means that the ***H***- and ***J***-aggregation are encouraged by nucleic acids. The ***H***- and ***J***-aggregation bands of MB in the presence of nucleic acids, located at 328 and 570 nm, respectively, are in agreement with the newly formed RLS peaks of the MB·DNA complex located 335.0 and 560 nm. Considering the appearance of the 472.0 nm RLS peak for the MB solution (Fig. 1) and ctDNA solution (Fig. 2), together with the RLS signals in the same wavelength region, which our former studies have reported,[31—37] it occurs to us that the RLS peak in the range of 470 nm is possibly the line emission of the xenon lamp in this area, because the intensity of the line emission of the xenon lamp is strong and may lead to a much stronger RLS.[34] The decrease in the RLS signals in the range lower than 308 nm with increasing MB concentration, which leads to an equal scattering point at 308.0 nm, is due to the strong absorption band at 292.5 nm.

Effects of the State of Nucleic Acids. It was found that the ***J***- and ***H***-aggregations of MB in the presence of nucleic acids depend on the pH, ionic strength and stranded structure of nucleic acids. Figure 6 shows that the intensity of RLS is stable in the pH range 6.87—8.74, and that any pH value out of the range produces a decrease in the RLS intensity. It is possible that the decrease in RLS intensity is due to the state change of nucleic acids when pH is lower than 6.87. In this acidity region, an indirect proton–phosphate interaction via water, and the protonation of nitrogen atoms of bases occur. For example, the protonation of cytosine N-3 (pK_a 4.24), and adenine N-1 sites (pK_a 3.20) occurs at pH 5.3, while guanine N-7 (pK_a 2.30) is protonated at pH < 3.[46] Thus, the dependence of the intensity of RLS on the pH of the medium reflects the state change of nucleic acids.

Similarly, the ionic strength affects the intensity of RLS. As Fig. 7 shows that the intensity of RLS is very sensitive to any change in the ionic strength. If the ionic strength is higher than 0.01, the RLS signals decrease rapidly. The effect of the ionic strength comes from the increasing stability of the double helix of nucleic acids with increasing ionic strength. As a controller of the ionic strength of the solution, Na^+ acts as a counter ion to reduce the unwinding tendency, which is due to an electrostatic repulsion between the negatively charged phosphate groups on adjacent nucleotides. Thus, the ionic strength controller also leads to a change in the state of nucleic acids.

Incubated in a boiling water-bath, double stranded DNA will be thermally denatured. As Fig. 8 shows, with increasing incubation time, the intensity of RLS decreases. Since thermal denaturation of double stranded nucleic acids produces single stranded nucleic acids, it is reasonable to infer

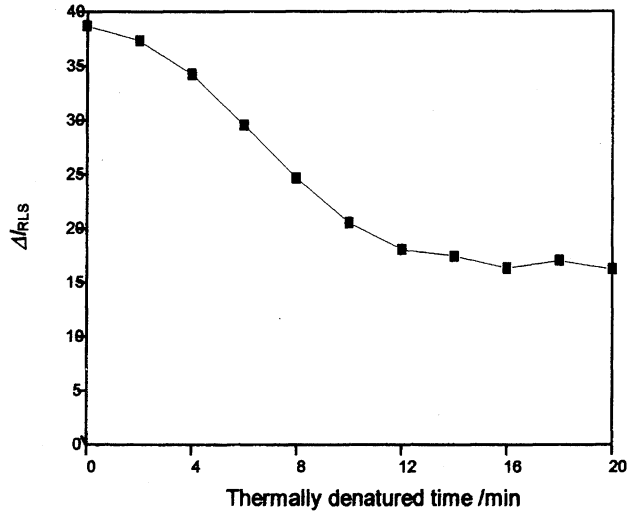

Fig. 8. The effects of thermally denature of nucleic acids on the intensity of RLS. Concentrations: MB, 3.0×10^{-5} mol dm^{-3}; ctDNA, 1.0 μg ml^{-1}. pH 8.14; ionic strength: 0.006.

that the interactions of MB with nucleic acids depend on the double stranded-structure of nucleic acids.

Nature of the Interactions of MB with Nucleic Acids. As the spectral characteristics of the interactions in terms of the RLS and electronic absorption spectra show, the interactions of MB with nucleic acids involve in two aggregation processes simultaneously, namely the ***H***- and ***J***-aggregations of MB in the presence of nucleic acids. Both processes depend on the pH and ionic strength of the solution, as well as on the double-stranded structure of nucleic acids. Since the present research involves a high *m* ratio, weak cooperative binding occurs under conditions where MB is in excess; thus the external stacking of MB on the molecular surface of nucleic acids takes place, and does not involve intercalative or groove binding.[27] It is therefore possible that the RLS enhancement effect of nucleic acids on MB results from the long-range assembly of organic dyes on the molecular surface of nucleic acids.[46] The ***H***- and ***J***-aggregation of MB in the presence of nucleic acids is essentially the long-range assembly of the organic dye organized on the molecular surface of the nucleic acids. The long range assembly, in which process nucleic acids act as templates, does not involve the groove or intercalative binding of organic dyes with nucleic acids.[46] Thus, the long-range assembly of MB only takes place on the molecular surface of nucleic acids, which produces large assembly products in size; therefore, enhanced RLS can be sensitively observed.

Tolerance of Foreigh Substances. The influence of various ions, proteins, sugars, surfactants, bases and nucleotides was tested at pH 8.14 and ionic strength 0.006 according to the standard procedure. The results are listed in Table 2. Of the ions, NH_4^+, K^+, Ca^{2+}, and Mg^{2+} can be allowed with higher concentration levels. Since they are hard ions, just like Na^+,[47] NH_4^+, K^+, Ca^{2+}, and Mg^{2+}, tend to bind almost exclusively to the phosphate groups of nucleic acids, stabilizing the Watson–Crick double stranded helix; thus their effects on the long-range assembly of MB are related to the shielding effects of counter ions on the negative backbone of nucleic acids. In contrast, soft ions, such as Hg^{2+}, which appears to bind exclusively with the base moiety of nucleic acids to form internal chelates, interstrand complexes or cross-links,[47] can be allowed at lower concentration levels. Borderline ions, such as Co^{2+} and Zn^{2+}, since they can bind either a phosphate group or the base moiety of nucleic acids, are comparatively allowed at higher concentration levels than that of soft ions. Even so, since the binding of metal ions with nucleic acids depends on the pH and ionic strength, the tolerance levels listed in Table 2 are not strictly in agreement with the binding rule.[47] Since the weak RLS signal of yRNA concerns the assembly, it was tested acting as a interference component.

Surfactants, such as SDS, CTMAB, zeph, gelatin, Triton X-100, β-CD and sugars can be allowed at higher levels, but they do not show any tendency to induce the aggregation of MB. Proteins can also be allowed at higher concentration levels, which supplies this assay with the possibility to determine the content of nucleic acids in practical samples. The high tolerant level of the base and nucleotide using this method supports our mechanism in view of the long-range assembly of MB on the molecular surface of nucleic acids.

Table 2. Tolerance of Foreign Substances

Substances	Concentration/mol dm^{-3}	Change of I_{RLS}/%
Al(III), SO_4^{2-}	18.5	−5.4
Ca(II), Cl^-	400.0	+7.7
Cd(II), Cl^-	1.00	−5.2
Co(II), Cl^-	5.0	+1.3
Cr(III), Cl^-	10.0	−6.8
Hg(II), NO_3^-	0.005	−8.6
K(I), Cl^-	5000	+9.5
Mg(II), Cl^-	400	−2.7
Mn(II), Cl^-	0.03	+2.3
NH_4^+, Cl^-	6700	+7.7
Pb^{2+}, Cl^-	1.93	+4.2
Zn^{2+}, Cl^-	3.06	−1.9
Glucose	2.0	+5.5
Lactose	0.25	+1.6
Maltose	0.25	−9.9
Sucrose	1.0	+6.9
β-Cyclodextrin	50.0[a)]	+0.4
Gelatin	0.5[a)]	+0.4
Triton X-100	0.4[b)]	+7.2
CTMAB	2.5	+2.7
SDS	2.5	+3.4
Protein, BSA	1.0[a)]	+3.6
Protein, HSA	1.0[a)]	+5.6
5′-AMP	0.50	+5.1
5′-GMP	0.50	+2.7
5′-CMP	0.50	+4.4
5′-UMP	0.50	+5.1
yRNA	19.3	+6.3
SO_4^{2-}	321.0	−7.7
PO_4^{3-}, Na^+	120.0	−5.6

a) and b) in the table are represented by μg ml^{-1} and %, respectively. Concentrations: MB, 3.0×10^{-5} mol dm^{-3}; ctDNA, 3.0×10^{-6} mol dm^{-3}. pH 8.14. Ionic strength 0.0045.

Table 3. Analytical Parameters of the Determination

Nucleic acids	Concentration of MB/10^{-5} mol dm^{-3}	Linear range $\mu g\ m^{-1}$	Linear regression equation (c, $\mu g\ ml^{-1}$)	LOD[a] 3σ/ng ml^{-1}	Correlation coefficient (r)
ctDNA	2.0	0—0.4	$\Delta I_{RLS} = -0.1 + 36.3c$	4.1	0.9999 ($n = 5$)
	3.0	0—1.2	$\Delta I_{RLS} = 2.8 + 35.7c$	4.2	0.9920 ($n = 7$)
	4.0	0—1.4	$\Delta I_{RLS} = 2.4 + 40.7c$	11.0	0.9961 ($n = 8$)
fsDNA	3.0	0—1.2	$\Delta I_{RLS} = 1.2 + 30.8c$	4.9	0.9987 ($n = 7$)
yRNA	3.0	0—0.24	$\Delta I_{RLS} = 0.1 + 17.5c$	8.6	0.9992 ($n = 4$)

a) Limit of determination. All the data were obtained by using 10.0 $\mu g\ ml^{-1}$ nucleic acid solution. pH 8.14. Ionic strength 0.006.

Table 4. Determination Results for Synthetic Samples

Nucleic acids in samples/$\mu g\ ml^{-1}$	Main additives[a]	Found value ($\mu g\ ml^{-1}$, $n = 5$)	Recovery range ($n = 5$)	RSD[b] %
ctDNA 25.0	BSA, SDS, β-CD	25.6	90.4—98.7	2.9
ctDNA 15.0	Co(II), Ca(II), Hg(II), NH_4^+	14.2	89.6—107.3	4.1
fsDNA 25.0	BSA, SDS, β-CD	24.7	92.1—105.1	3.1
fsDNA 15.0	5′-AMP, 5′-GMP, 5′-CMP, $H_2PO_4^-$	15.4	91.3—105.5	2.5

a) Concentrations of additives: BSA, 0.1 $\mu g\ ml^{-1}$; nucleotide and $H_2PO_4^-$: 5.0×10^{-5} mol ml^{-1}; Co^{2+}: 2.0×10^{-8} mol dm^{-3}; Ca^{2+}: 2.0×10^{-5} mol dm^{-3}; NH_4^+: 1.3×10^{-4} mol dm^{-3}; Hg^{2+}: 2.0×10^{-10} mol dm^{-3}; SDS: 5.0×10^{-8} mol dm^{-3}; β-CD: 1.0×10^{-6} mol dm^{-3}. pH: 8.14; ionic strength: 0.006. b) Relative standard deviation for 5 measurements.

Calibration Curves and Determination of Samples. Under optimal conditions according to standard procedures, the calibration curves of ctDNA, fsDNA, and yRNA were constructed with increasing the concentrations of nucleic acids. There are linear relationships between the intensity of RLS and the concentration of nucleic acids. All of the analytical parameters have been regressed, and are presented in Table 3. In terms of the slope of the regression equations, the sensitivities of RLS method have the sequence for the three tested nucleic acids: ctDNA > fsDNA > yRNA. Table 3 shows that yRNA has a short linear range and low sensitivity, which indicates that this method is not appropriate to a yRNA determination. However, the weak signal of the interaction of MB with yRNA shows the dependence of the interaction on the double-stranded structure of nucleic acids.

Besides the effects of the concentration of MB on the RLS spectra in the molecular absorption region (Fig. 2), the concentration of MB has effects on the linear range of determination (Table 3). By using different concentrations of MB, since we can obtain an appropriate linear range, the determination of nucleic acids can be established according to the reality. To test the method, four synthetic samples, which were constructed based on the interferences of foreign substances (Table 2), were determined according to the results given in Table 3. As Table 4 shows, the results are reproducible and reliable.

Conclusion

The ***H***- and ***J***-aggregation of MB occurs in the presence of nucleic acids. A mechanism study shows that the ***H***- and ***J***-aggregation are essentially the long-range assembly of MB on the molecular surface of nucleic acids. The long-range assembly depends on the pH, ionic strength, and stranded structure of nucleic acids. Based on the long-range assembly, which results in a markedly enhanced RLS, nucleic acids of nanogram levels can be determined. Since of all the data are obtained by using a common spectrofluorometer, this method is simple, sensitive and practical.

This project has received the supports from the National Natural Science Foundation of China (NSFC, No. 29875019) and the Municipal Science Foundation of Chongqing for Young and Middle Scientists (No. 97-4729). All of the authors express their deep thanks.

References

1 Y. J. Wei, S. Y. Tong, and K. A. Li, *Acta Chim. Sin.*, **53**, 83 (1995).

2 I. Hag, I. O. Trent, B. Z. Chowdhry, and T. C. Jenkins, *J. Am. Chem. Soc.*, **121**, 1768 (1999).

3 P. A. Piuno and U. J. Krull, *Anal. Chem.*, **67**, 2635 (1995).

4 C. Z. Huang, K. A. Li, and S. Y. Tong, *Anal. Chim. Acta*, **345**, 235 (1997).

5 C. Z. Huang, Y. F. Li, and H. Q. Luo, *Anal. Lett.*, **31**, 1149 (1998).

6 R. E. Sheridan, C. M. O'Donnell, and E. R. Pautler, *Anal. Biochem.*, **52**, 657 (1973).

7 R. Marqut and E. Rosenbery, *Anal. Biochem.*, **176**, 265 (1989).

8 G. J. Gendimenico, P. L. Bouquin, and K. M. Tramposch, *Anal. Biochem.*, **173**, 45 (1988).

9 R. W. Hubbard, W. T. Matthew, and D. W. Moulton, *Anal. Biochem.*, **46**, 461 (1972).

10 R. F. Martin and D. C. Donohue, *Anal. Biochem.*, **47**, 562 (1972).
11 A. N. Glazer and H. S. Rye, *Nature (London)*, **359**, 589 (1992).
12 M. V. Lankecker and L. C. Ghyssens, *Anal. Lett.*, **19**, 615 (1986).
13 J. Rao and W. R. Otto, *Anal. Biochem.*, **207**, 186 (1992).
14 H. S. Rye, M. A. Quesada, K. Peck, R. A. Mathies, and A. N. Glazer, *Nucl. Acids Res.*, **19**, 327 (1991).
15 J. T. Petty, M. E. Johnson, P. M. Goodwin, J. C. Martin, J. H. Jett, and R. A. Keller, *Anal. Chem.*, **67**, 1775 (1995).
16 B. B. Haab and R. A. Mathies, *Anal. Chem.*, **67**, 3253 (1995).
17 M. D. Topal and J. R. Fresco, *Biochemistry*, **19**, 5531 (1980).
18 Y. X. Ci, Y. Z. Li, and W. B. Chang, *Anal. Chim. Acta*, **248**, 589 (1991).
19 Y. X. Ci, Y. Z. Li, and X. J. Liu, *Anal. Chem.*, **67**, 1785 (1995).
20 C. Z. Huang, K. A. Li, and S. Y. Tong, *Chin. J. Anal. Chem.*, **25**, 759 (1997).
21 C. Z. Huang, Y. F. Li, K. A. Li, and S. Y. Tong, *J. Chin. Rare Earth Soc.*, **16**, 84, (1998).
22 C. Z. Huang, K. A. Li, and S. Y. Tong, *Chemistry (Chin. Chem. Soc., Taipei)*, **55**, 1, (1997).
23 C. Z. Huang, K. A. Li, and S. Y. Tong, *Mikrochim. Acta*, **126**, 231 (1997).
24 C. Z. Huang, K. A. Li, and S. Y. Tong, *Anal. Lett.*, **29**, 1705 (1996).
25 C. Z. Huang, Y. F. Li, K. A. Li, and S. Y. Tong, *Anal. Lett.*, **30**, 1305 (1997).
26 E. Tuite and J. M. Kelly, *Biopolymers*, **35**, 419 (1995).
27 E. Tuite, J. M. Kelly, G. S. Beddard, and G. D. Reid, *Chem. Phys. Lett.*, **226**, 517 (1994).
28 G. A. Miller, *J. Phys. Chem.*, **82**, 616 (1978).
29 R. F. Pasternack, C. Bustamante, P. J. Collings, A. Giannetteo, and E. J. Gibbs, *J. Am. Chem. Soc.*, **115**, 5393 (1993).
30 R. F. Pasternack and P. G. Collings, *Science (Washington D. C.)*, **269**, 935 (1995).
31 Y. F. Li and C. Z. Huang, *Chin. J. Anal. Chem.*, **26**, 1508 (1998).
32 C. Z. Huang, K. A. Li, and S. Y. Tong, *Anal. Chem.*, **68**, 2259 (1996).
33 C. Z. Huang, K. A. Li, and S. Y. Tong, *Anal. Chem.*, **69**, 514 (1997).
34 C. Z. Huang, Y. F. Li, and X. D. Liu, *Anal. Chim. Acta*, **375**, 89 (1998).
35 C. Z. Huang, Y. F. Li, J. G. Mao, and D. G. Tan, *Analyst*, **123**, 1406 (1998).
36 C. Z. Huang, J. X. Zhu, K. A. Li, and S. Y. Tong, *Anal. Sci.*, **13**, 263 (1997).
37 C. Z. Huang, K. A. Li, and S. Y. Tong, *Bull. Chem. Soc. Jpn.*, **70**, 1843 (1997).
38 C. Z. Huang, K. A. Li, and S. Y. Tong, *Chem. J. Chin. Univ.*, **18**, 525 (1997).
39 C. Z. Huang, Y. F. Li, N. Li, K. A. Li, and S. Y. Tong, *Bull. Chem. Soc. Jpn.*, **71**, 1791 (1998).
40 C. Z. Huang, Y. F. Li, and X. H. Huang, *Acta Phys.-Chim. Sin.*, **14** (**8**), 731 (1998).
41 Z. Y. Chen, J. Liu, and D. Luo, "Biochemical Experiments," Hefei, China (1994), p. 111.
42 Y. E. Zeng, H. S. Zhang, and Z. H. Chen, "Handbook of Modern Chemical Reagents," Chemical Industry Press, Beijing (1989), Vol. 4, p. 793.
43 D. L. Akins, H. R. Zhu, and C. Guo, *J. Phys. Chem.*, **98**, 3612 (1994).
44 G. Satchard, *Ann. N. Y. Acad. Sci.*, **51**, 660 (1949).
45 K. G. Strothkamp and R. E. Strothkamp, *J. Chem. Educ.*, **71**, 77 (1994).
46 M. J. Carlvin, N. Datta-Guputa, and R. J. Fiel, *Biochem. Biophys. Res. Commun.*, **108**, 66 (1992).
47 K. B. Jacobson and J. E. Turner, *Toxicology*, **16**, 1 (1980).